Cell Stress and Chaperones (2024) 29:338–348
https://doi.org/10.1016/j.cstres.2024.03.008

Autorepression of yeast Hsp70 cochaperones by intramolecular interactions involving their J-domains

Mathieu E. Rebeaud[1,2] · Satyam Tiwari[2] · Bruno Fauvet[2] · Adelaïde Mohr[2] · Pierre Goloubinoff[1,*] · Paolo De Los Rios[2,3,*]

Received: 9 February 2024 / Revised: 19 March 2024 / Accepted: 19 March 2024

Abstract

The 70 kDa heat shock protein (Hsp70) chaperones control protein homeostasis in all ATP-containing cellular compartments. J-domain proteins (JDPs) coevolved with Hsp70s to trigger ATP hydrolysis and catalytically upload various substrate polypeptides in need to be structurally modified by the chaperone. Here, we measured the protein disaggregation and refolding activities of the main yeast cytosolic Hsp70, Ssa1, in the presence of its most abundant JDPs, Sis1 and Ydj1, and two swap mutants, in which the J-domains have been interchanged. The observed differences by which the four constructs differently cooperate with Ssa1 and cooperate with each other, as well as their observed intrinsic ability to bind misfolded substrates and trigger Ssa1′s ATPase, indicate the presence of yet uncharacterized intramolecular dynamic interactions between the J-domains and the remaining C-terminal segments of these proteins. Taken together, the data suggest an autoregulatory role to these intramolecular interactions within both type A and B JDPs, which might have evolved to reduce energy-costly ATPase cycles by the Ssa1–4 chaperones that are the most abundant Hsp70s in the yeast cytosol.

Keywords DNAJA · DNAJB · Autorepression · Coevolution · JDPs

Introduction

During *de novo* folding and under stress, many native proteins may transiently denature, readily misfold, and form stable aggregates lacking their specific dedicated biological activity.[1] Misfolded species can be cytotoxic and, in humans, are associated with several neurodegenerative disorders, such as Alzheimer's and Parkinson's diseases.[2] Early in Life's history, the first prokaryotes evolved a complex protein quality control network comprising several

Abbreviations: ATP, adenosinetriphosphate; BSA, bovineserum albumin; DnaJA, DnaJhomolog subfamily A; DnaJB, DnaJhomolog subfamily B; DNAJB1, DnaJhomolog subfamily B member 1; DNAJB6, DnaJhomolog subfamily B member 6; DNAJB8, DnaJhomolog subfamily B member 8; DNAJA2, DnaJhomolog subfamily A member 2; DTT, dithiothreitol; DnaK, 70-kDaheat shock protein; EEVD, conservedC-terminal EEVD motif; FRET, Fluorescenceresonance energy transfer; G/F, glycine-phenylalanine-richregion; G6PDH, Glucose-6-phosphatedehydrogenase; Hsc70, heatshock cognate 70; Hsp40s, 40-kDaheat shock protein, also known as JDPs; Hsp60s, 60-kDaheat shock protein; Hsp90s, 90-kDaheat shock protein; Hsp100s, 100-kDaheat shock protein; Hsp110, Hsp110; IPTG, Isopropylβ-D-1-thiogalactopyranoside; JDP, J-domainprotein; MLucV, reporterchaperone substrate composed of a stress-labile luciferase flanked bystress-resistant fluorescent domains; pLDDT, predictedLocal Distance Difference Test; PDB, ProteinData Bank

* Pierre Goloubinoff
pierre.goloubinoff@unil.ch

* Paolo De Los Rios
paolo.delosrios@epfl.ch

[1] Department of Plant Molecular Biology, Faculty of Biology and Medicine, University of Lausanne, CH-1015 Lausanne, Vaud, Switzerland

[2] Institute of Physics, School of Basic Sciences, École Polytechnique Fédérale de Lausanne – EPFL, 1015 Lausanne, Vaud, Switzerland

[3] Institute of Bioengineering, School of Life Sciences, École Polytechnique Fédérale de Lausanne – EPFL, 1015 Lausanne, Vaud, Switzerland.

Published online: 21 March 2024

classes of proteins, including highly conserved molecular chaperones that can specifically target, bind, and thereby repair polypeptides that are conformationally compromised and highly conserved ATP-fueled chaperone-gated endocellular proteases that can specifically target, bind, and degrade potentially toxic polypeptides that became irreversibly misfolded.[1,3] Except for the small heat shock proteins (Hsps), the main chaperone families, Hsp100s, Hsp90s, Hsp60s, and 70 kDa heat shock proteins (Hsp70s) are ATPases that can use the energy liberated by ATP hydrolysis to remodel bound misfolded and aggregated protein substrates, ultimately leading to refolding to the native state. Among the ATPase chaperones, the Hsp70s have emerged as the central hub of the protein quality control network that coordinates the optimal unfolding of stably misfolded or alternatively folded protein species, leading to the proper refolding of native proteins, even under nonequilibrium conditions unfavorable to the native state.[3,4]

The triage of polypeptide substrates in need to be structurally altered/modified by Hsp70s is initially performed by their obligate J-domain protein (JDP) cochaperones.[5–7] JDPs feed Hsp70s with polypeptide substrates and promote the locking of Hsp70s onto the incoming polypeptide substrates that are, but not limited to, misfolded and/or aggregated. To catalyze polypeptide-uploading onto Hsp70 and trigger Hsp70's ATPase, all JDPs must therefore comprise at least two domains: one very diversified that can directly recognize or be colocalized with specific Hsp70 substrates and one remarkably conserved, the namesake J-domain (JD), that recognizes and binds Hsp70 molecules in their ATP-bound conformation much more strongly than when they are in the ADP-bound conformation.[8] JDs comprise ~65 residues, some of them highly conserved, like a characteristic His-Pro-Asp motif[9] known to specifically anchor into a pocket of the Hsp70-ATP complex in which it closely interacts with a folded interdomain linker between the protein-binding and nucleotide-binding domains of ATP-Hsp70 (see PDB 5NRO). In contrast, in the ADP-Hsp70 conformation, the JD does not interact with the unfolded interdomain chaperone linker that became exposed and unstructured[10] (see PDB 2KHO). The concomitant interaction with Hsp70 of a JD and a polypeptide substrate greatly accelerates Hsp70's ATPase cycle,[10–12] resulting in a nonequilibrium enhancement of the affinity of the chaperone for its substrates called ultra-affinity.[13]

Following denaturing stress, such as heat shock, conserved homodimeric class A and B JDPs (traditionally called Hsp40s, and in yeast Ydj1 and Sis1, respectively) predominantly bind to misfolded and aggregated proteins[5,6] by their two C-terminal domains (CTDs) (including the structurally poorly-resolved linkers with the JDs) and, at the same time, bind ATP-bound Hsp70s through their two N-terminal JDs. Owing to the high flexibility of G/F-rich linkers connecting the JDs to the CTDs, the JDs of both classes would be expected to freely swing and, thereby, seek unrestrained binding to ATP-Hsp70s. Yet, there is emerging evidence of intramolecular regulatory mechanisms that may reversibly block the interaction between the JDs of class B JDPs (yeast Sis1 and human DNAJB1) and the corresponding cytoplasmic Hsp70s (yeast Ssa1–4 and human Hsc70). In the case of Sis1, interactions between Glu-50 on JD and Arg-73 are documented on a short helical motif adjacent to the C-terminal of helix IV[14] (Figure S1), whose mutational disruption, or by swapping the JD of Sis1 for that of Ydj1, increases the ability of Sis1 to trigger the refolding activity of Ssa1.[14,15] It has also been reported that human DNAJB1 comprises a distal α-helix inside the G/F region (helix V, Figures S1 and S2, see sequences in Supplementary Data), whose deletion facilitates the cooperation of DNAJB1 with Hsc70 for refolding different misfolded substrates.[16,17] The CTDs of DNAJB1 also participate in this intricate network of interactions, as testified by the finding that the C-terminal EEVD motif of Hsc70, which interacts with the CTD1 subdomain of DNAJB1,[18,19] is necessary to alleviate the helix V-induced inhibition of DNAJB1's cochaperone activity, however through a mechanism yet not fully resolved structurally. Similar results have been obtained for yeast Sis1.[20] Furthermore, through a series of modular domain deletions or domain swaps with Ydj1, it has been shown in yeast that only chimeras containing the CTDs of Sis1 are effective in preventing prion propagation and toxicity, with their effectiveness depending to some extent on the origin of the JD and of the G/F region.[21] In contrast to Sis1, the presence of an intramolecular mechanism in Ydj1 that might tune the action of its JD has not been reported, despite AlphaFold2[22] predicting interdomain motifs similar to those of Sis1: two alfa-helices, one right following helix IV and another, although with lower reliability, within the G/F region (see pLDDT in Figure S3).[15,23,24] In addition to these examples, recent experimental studies have documented the interaction of the JD with other structural elements of the same polypeptide in various JDPs (e.g. DNAJB6, DNAJB8).[25,26] Adding to the richness of effects that are modulated by interactions between the JDs and other domains of JDPs, it was found that the ability of individual DNAJA or DNAJB homodimers to unlock the unfolding–refolding activity of Hsp70s is much higher when they are in the presence of one another, as compared to their stand-alone effects.[27]

In this work, we investigated the presence of intramolecular mechanisms by which the two main JDPs in yeast cytosol, Ydj1 (class A) and Sis1 (class B) (hereafter called YY and SS, respectively), regulate the activity of the main yeast cytosolic Hsp70, Ssa1. Inspired by previous works,[14,15,17,28,29] we developed two new chimeras,

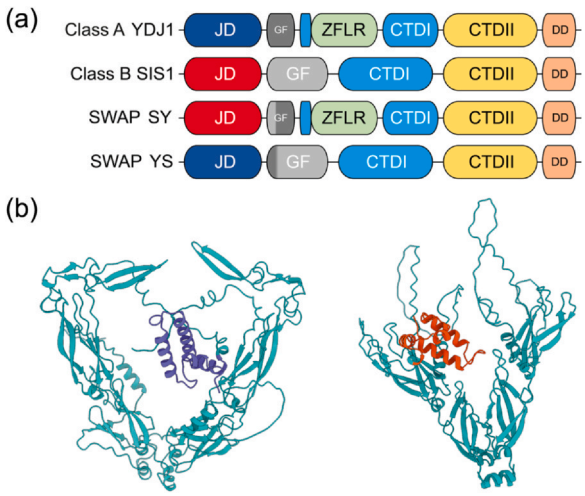

Fig. 1 Domain organization of yeast class A (YDJ1) and B (SIS1) JDPs and of the swap chimeras. (a) Domain organization of Sis1 and Ydj1. J-domain (JD), G/F-rich region (GF), dimerization domain (DD), Zinc-finger-like region (ZFLR). (b) Alphafold2 prediction of left: Class A (YY) and right: Class B (SS) with only one JD of each homodimer shown (complete model in Figure S2). For more clarity, the model of SS has been rotated 90° on the left compared to the one of YY. Abbreviations used: CTD, C-terminal domain; JDP, J-domain protein.

henceforth called YS and SY, obtained by swapping the JDs of YY and SS (with the first letter indicating the parent protein of the N-terminal JD and the second letter indicating the parent protein of the remaining part of the chimera sequence). Comparing the behavior of the two wild-type JDPs with that of the two chimeras across a series of assays (disaggregation and refolding of preaggregated enzymes, prevention of aggregation, and activation of Ssa1′s ATPase), we highlighted the presence of intramolecular interactions between the JDs, the G/F regions and the CTDs that likely offer cells a way to regulate their multiple Hsp70-dependent and JDP-dependent functions, and thus the energy-consuming cycles by their abundant Hsp70s, depending on cellular needs and on ATP availability.

Results

We designed the two chimeras by swapping the 80 N-terminal residues containing the JD domains and the first 10–12 residues of the G/F hinge region of Ydj1 and Sis1 (Figure 1, Supplementary Data for the detailed sequences). In the case of Sis1, the swap preserved the inhibiting E50–R73 interaction but abolished the interaction between the JD and helix V. The interactions observed here are derived from the AlphaFold2 predictions, but they are also shown in the crystal structure of 1–81 N-terminal fragment of Sis1 (PDB: 4RWU).

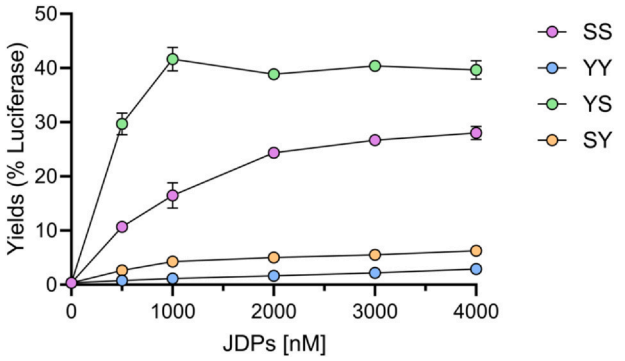

Fig. 2 Different refolding effectiveness of wild-type and chimeric JDPs. Efficiency of different JDPs proteins (SIS1 and YDJ1 and the two swap SY and YS) to power SSA1-mediated disaggregation of heat-urea preaggregated Luciferase. 0.2 μM of stable inactive luciferase aggregates were incubated for up to 120 min at 25 °C in the presence of 5 mM ATP, 6 μM of SSA1, 0.75 μM SSE1, and between 0 and 4 μM of either YY, SS, SY, or YS. In all panels, error bars represent mean ± SD (n = 3). Abbreviations used: JDP, J-domain protein; SD, standard deviation.

We then tested the *in vitro* ability of increasing concentrations of YY, SS, YS, and SY to drive the native refolding of stable, preformed urea- and heat-preaggregated luciferase[30] by a constant amount of Ssa1 and Sse1 (the yeast member of the Hsp110 family). Sse1, in the presence of ATP, is considered to act both as a nucleotide exchange factor and as a disaggregating cochaperone (Figure 2). Remarkably, at all concentrations, YS was found to be much more effective at promoting the refolding preaggregated luciferase by Ssa1 than wild-type SS, with a more marked difference at low concentrations. Similarly, SY was more effective than YY, although both were much less effective than SS. The action on different substrates, preformed heat-aggregated G6PDH and MLucV,[31] showed a similar pattern (Figures S4 and S5). We also tested the refolding ability of the JDPs with a mutant of Ssa1 in which the last four C-terminal amino acids have been deleted (ΔEEVD, Figure S6) since it has been previously established that the EEVD motif regulates SS activity.[14,20] Expectedly, Sis1 (SS) was totally unable to drive the refolding of preaggregated luciferase by the ΔEEVD mutant, but also YY and SY were partially inhibited when compared to their efficiency with wild-type Ssa1. Instead, the effect of Ssa1′s C-terminal EEVD deletion was only very mild on the action of YS, which has the JD of YY, although it contained a type B CTD that has been reported to bind the EEVD peptide.[14,32] This result is in line with previous works where the JD from Sis1 was swapped with the ones of Ydj1 and Xdj1,[14,33] in which nonetheless the E50–R73 interaction was lost, at variance with the present domain swap. Thus, the relief of JDP autorepression is sufficient in our experiments to rescue the disaggregation activity of

Hsp70 even in the absence of EEVD, a result, which is nonetheless in contrast with the role of EEVD for α-synuclein fibril disaggregation by the human DNAJB1–HSC70 system that in contrast stringently depends on EEVD.[16]

To explain the observed ranking of effectiveness, it was necessary to invoke some functional interaction between the JDs and the CTDs. Indeed, the independent-domain assumption could explain the greater yield of YS compared to SS by positing that the JD of YY was more effective than the JD of SS at recruiting and activating Hsp70, while the CTD of SS was more effective than the CTD of YY at capturing the substrate and delivering it to Hsp70. Yet, a direct extension of this argument would have predicted that SY, which would have comprised the least effective instance of each domain, should have been the least efficient of the four constructs, contrary to our findings. The independent action hypothesis can thus be excluded, and intramolecular interactions between the JDs and the CTDs were required to explain the results.

We thus addressed more in detail the effects of the JD swap on the two functions usually ascribed to the two domains: stimulation of the ATPase cycle of Ssa1 by the JDs and substrate binding by the CTDs (including most of the G/F linker and, in the case of Ydj1, also the cysteine-rich domain).

To test substrate binding by SS, YY, YS, and SY, we measured their specific ability to block the increase of the light-scattering signal of aggregating, urea-preunfolded luciferase (see Materials and methods and Figures S7 and S8 for a characteristic time-course of aggregation). Consistent with the literature, different doses of YY were found to be more effective at reducing protein aggregation than SS.[15,34] Comparing the swap mutants with the wild-types, we observed, in several assays and for different aggregating substrates, that SY systematically prevented aggregation more efficiently than YY (Figures 3, S7, and S8). These results offered insights into the intramolecular interactions of these JDPs. Barring the unlikely possibility that the JD of YY could by itself bind substrates, a feature that has never been reported, the differences found between YY and SY suggested that intramolecular interactions between the JD of YY and its CTD partially interfered with the ability of the YY CTDs to engage aggregating polypeptide substrates. In contrast, in the SY chimera, the JD of SS has not coevolved and therefore is not expected to have transient interactions with YY's CTDs, allowing them to freely bind misfolding substrates and prevent their aggregation. In contradistinction, the reverse chimera, YS, was only marginally, if at all, worse than SS at preventing substrate aggregation (see Figure S9 for additional substrate), indicating that any intra-SS JD/CTD interactions, if present, do not interfere with substrate binding. While the differences in substrate-binding efficiency between SS and YY have already been reported elsewhere, the role of their JDs in competing with misfolded substrates for the CTDs has not been previously reported, and in particular, they hint at relevant JD–CTD interactions in the case of YY.

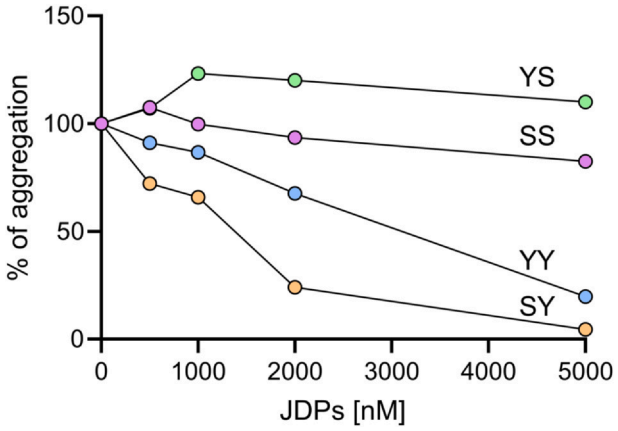

Fig. 3 J-domain protein acting as holding chaperone. Efficiency of SS, YY, SY, and YS at preventing luciferase aggregation. 10 μM Luciferase was preunfolded with 6 M urea at 30 °C for 30 min, then diluted to a final concentration of 0.3 μM in buffer (50 mM Tris-HCl pH 7.5, 150 mM KCl, 10 mM $MgCl_2$, 2 mM DTT), in the absence or in the presence of increasing concentrations of YY, SS, SY, YS. Relative aggregation yields following 800 s were calculated in the presence of increasing concentrations of YY, SS, SY, YS. Maximal aggregation without JDPs at 800 s was set to 100%. The time-dependent aggregation was monitored by light scattering at 340 nm at 30 °C. Abbreviation used: JDP, J-domain protein.

To test the second relevant role of JDPs, namely stimulation of the ATPase cycle of Hsp70, we measured the rates of ATP hydrolysis by Ssa1 in the presence of increasing concentrations of the four JDPs (Figure 4(a)) and, as a reference, we also measured the ATPase rates in the presence of the same increasing concentrations (protomer by protomer) of isolated JDs.

No major differences were found in the effects of the isolated JDs of YY and SS, indicating that their ability to interact with Ssa1 and to stimulate its ATPase activity is similarly low (Figure 4(a)). The effects of the two swap chimeras, YS and SY, were also similar, albeit a much higher ATPase stimulation in their presence compared to the isolated JDs, suggesting that some parts of the full-length JDPs different from the isolated JDs might also act as Ssa1 substrates,[10,35] thereby synergistically stimulating Ssa1's ATPase. The wild-types YY and SS had intermediate effects, between those of isolated JDs and those of the swap chimeras. SS was systematically less effective than both chimeras, indicating that its JD was also in an inactive state that affected the ability of

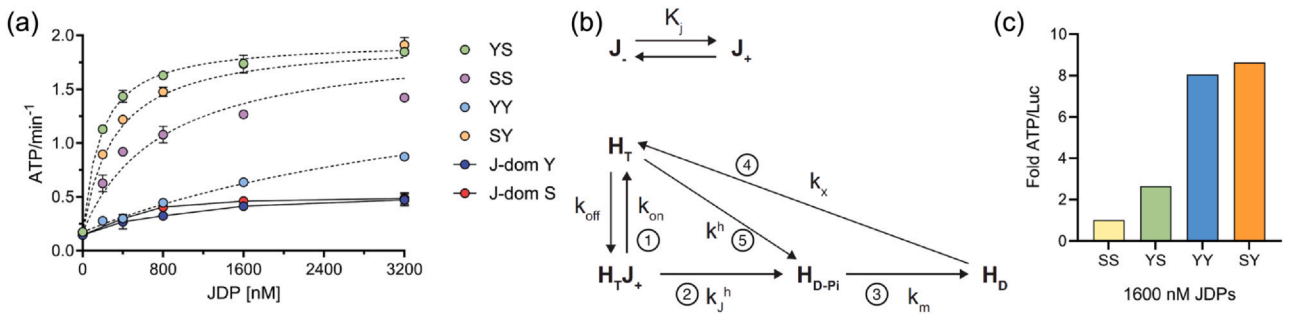

Fig. 4 ATPase activity of Ydj1, Sis1, and of their J-domain swapped chimeras. (a) Rates of ATP hydrolysis of 6000 nM SSA1 and 750 nM SSE1 without substrate in the presence of increasing concentrations of YY, SS, YS, and SY. (b) Reaction scheme for the activation of the ATPase cycle of Ssa1 by the different Hsp40 constructs. (c) Fold-change of ATP hydrolyzed per natively refolded luciferase with SIS1 set as a reference, by 6000 nM SSA1 and 750 nM SSE1, in the presence of either 1600 nM YY, SS, SY, or YS. The error bars in panels A represent mean ± SD (n = 3). Abbreviations used: JDP, J-domain protein; SD, standard deviation.

SS to activate Ssa1. Instead, YY was more effective than isolated JDs only at the highest tested concentrations and was always much less effective than SS. Since the JDs of Ydj1 and Sis1 were similarly effective both when isolated and when swapped, the decreased effectiveness of wild-type YY and SS suggested that intramolecular interactions between their respective JDs and the CTDs were inhibiting their ability to freely interact and activate Ssa1's ATPase. This autorepression was particularly strong in the case of YY.

We modeled these data by means of the reaction schemes in Figure 4(b). YY and SS are in a dynamical equilibrium between the autorepressed and active states (J_- and J_+, respectively), characterized by an equilibrium constant K_J, associated with the relation $[J_+] = K_J [J_-]$ (red reaction): K_J values smaller than 1 mean that the JDP is most likely found autorepressed. The subsequent reactions are: (1) Ssa1 bound to ATP (H_T) can only bind to and unbind from J_+, with JDP association and dissociation rates k_{on} and k_{off}; (2) following JDP association, ATP hydrolysis is induced with rate k_J^h, resulting in Ssa1 bound to ADP and inorganic phosphate ($H_{D\text{-}Pi}$); (3) the ensuing release of inorganic phosphate with rate k_m results in Ssa1 bound only to ADP (H_D); this reaction is followed by (4) ADP-to-ATP exchange with a rate k_x; in parallel to the JDP-stimulated hydrolysis pathway, (5) Ssa1 can also hydrolyze ATP spontaneously, albeit at a much slower rate k^h. We simplified the scheme for the swap chimeras with the assumption that they are never autorepressed (due to the presumed absence of complementary surfaces on their JD and CTD, that in wild-type SS and YY would have coevolved to specifically interact to form the autorepressed state), and that thus no J_- state is present. The analytical solution of these reactions provides formulas for the steady-state ATPase rate that we used to fit the experimental data (Figure 4(a), dashed lines). While the fits were not perfect, due to some simplifications in the model and to the potential presence of unknown features of the system that we were not capturing, they were nonetheless instructive. The main result of this analysis was that in both wild-types, the equilibrium was tilted toward the autorepressed state ($K_J < 1$), much more strongly in YY ($K_J \approx 1/30$) than in SS ($K_J \approx 1/2$). This result further supported the hypothesis that intramolecular interactions in YY and SS, involving the JD, may partially sequester the JD and/or the parts of the JDP that could act as Ssa1 substrates.

Table 1
Summary of the functional efficiencies of the JDPs.

JDP	Efficient at holding	Efficient for Ssa1 ATPase	Efficient at refolding
YY	✓	✗	✗
SS	✗	✓	✓
YS	✗	✓✓	✓✓
SY	✓✓	✓✓	✗

Abbreviation used: JDP, J-domain protein.

An ancillary observation from Figure 4(a) is that in all cases, apart from YY, saturation of the Ssa1 ATPase activity was achieved by amounts of JDP or of isolated JDs that were substoichiometric to Ssa1. Within our reaction scheme (Figure 4(b)), this is a consequence of the overall exchange rate (namely, the release of Pi and ADP-to-ATP exchange), which was much slower than the rate of ATP hydrolysis and of the ensuing release of the JD. This implies that, in the absence of a nucleotide exchange factor, a single JD acts catalytically, activating several Ssa1s before the first one undergoes nucleotide exchange and resets its cycle.[10] This is consistent with proteomic data estimating the presence in the yeast cytosol of seven times more Ssa1–4 (together ~14 μM protomers) than of YY and SS (together ~2 μM protomers).[36–38] We summarized these findings in Table 1.

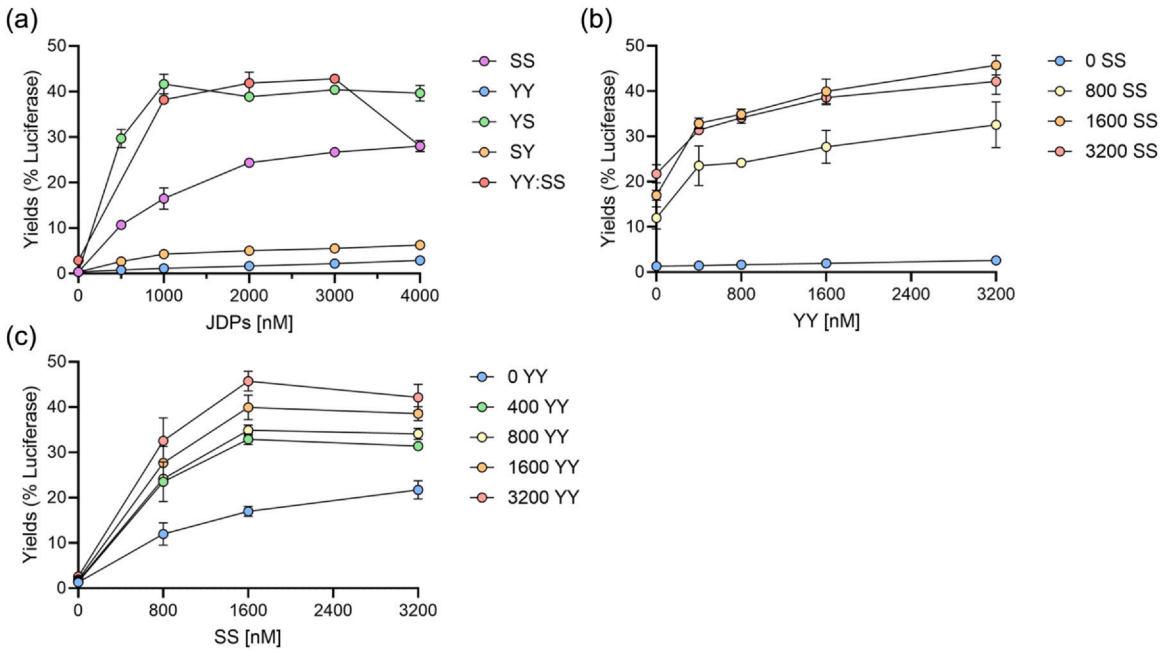

Fig. 5 Synergistic action of Ydj1 and Sis1. (a) Data as in Figure 2, together with data for the measured yields of refolded luciferase achieved by a x%/(100 − x)% mixture of SS and YY respectively. The simple sum of the two contribution is in dashed line. (b) Dose response of YY for fixed amounts of SS to refold preaggregated luciferase. (c) Dose response of SS for fixed amounts of YY to refold preaggregated luciferase. The error bars in panels B and C represent mean ± SD (n = 3). Abbreviations used: JDP, J-domain protein; SD, standard deviation.

The addition of a true substrate (preaggregated luciferase) further increased all ATPase rates 1.5–1.7-fold for all full-length JDP constructs (Figure S10). Combining these data with those shown in Figure 2(a), we estimated the relative ATP cost of the *in vitro* disaggregation/refolding reaction in the presence of a constant amount (1600 nM) of SS, YY, YS, or SY (Figure 4(c)). The most energy-efficient JDP of the four constructs was SS (whose relative efficiency was set to 1). The second most energy-efficient JDP was YS, which nevertheless hydrolyzed 2.6 times more ATPs per refolded Luciferase, while YY and SY were equally energy inefficient, hydrolyzing at least eight times more ATP per refolded luciferase than SS. Thus, the constructs with the CTDs of Ydj1 were both slower at refolding preaggregated luciferase, and less efficient at using ATP energy.

In metazoa, as well as in yeast, the disaggregation and subsequent refolding of luciferase aggregates is enhanced by the synergistic coaction of homodimeric class A and B JDPs, likely mediated by intermolecular interactions between JDs and CTDs of different classes.[20,27] We first confirmed these results, finding that in our assays, a mixture of SS and YY at constant total JDP concentration was more effective than the sum of their individual contributions (Figure 5(a)). We observed that the YS chimera and the YY:SS mixture had very similar behavior as for equal YS and SS concentrations, hinting at a role of the synergy in activating the JDs. The data in Figure 5(a) also suggested that the synergy between SS and YY may be catalytic: small amounts of each could greatly enhance the activity of the other, making them maximally active. We confirmed that interpretation by measuring the effects of increasing concentrations of YY (SS) on fixed amounts of SS (YY) (Figures 5(b), (c), and S11(a)). In both cases, small amounts of one JDP were able to greatly enhance the activity of the other.

We also analyzed the mutual activatory role of the two chimeras by adding an increasing quantity of YS to a decreasing quantity of SY, at a fixed total 4000 nM concentration. We found the refolding efficiency of the mixture was not greater than the simple sum of their individual efficiencies (Figure S11(a) for the wild-type mixture and B for the mixture of swap chimeras). The absence of synergy upon domain swapping strengthens the hypothesis that the JDs play a crucial intermolecular role in making the YY and SS interact, confirming, through a different angle, previous results.[27]

Discussion

There is emerging evidence that intramolecular dynamic interactions in some JDPs might have a role in reducing unnecessary interactions with Hsp70s, for example, when there is no stress and very little protein aggregation, and thereby possibly avoiding futile ATP hydrolysis in unstressed cells, by maintaining partially sequestered their J-domains. This is evocative of a Swiss army knife, whose

blade can either be autorepressed, with its blade folded in its handle, or derepressed with its blade exposed and poised to perform its cutting function. Our data suggest that both DnaJAs and DnaJBs can either be autorepressed, with their JDs interacting with their CTDs, or derepressed with their JDs exposed and free to bind and activate Hsp70. Whereas in the absence of substrates to be cut the purpose of the knife's autorepression is security, it is tempting to speculate that in the absence of a substrate to be unfolded JDP's autorepression may be to reduce unnecessary futile ATP hydrolysis by the Hsp70s. Unstressed Escherichia coli cells may contain up to 30 micromolar DnaK,[39] which if left untamed could waste between 1.8 and 18 mM ATP in 1 h. Similarly, when deprived of an energy source, full Hsp70 activation also could become an acute problem for quiescent unstressed yeast cells containing around 15 micromolar SSA1–4.[36–38]

In the case of human DNAJB1, a class B JDP implicated in protein refolding and disaggregation, autorepression has been ascribed to two intramolecular structural elements: a contact between E50 and K73 (E50 and R73 in yeast Sis1, relevant for the present work) and a more extensive interaction, which was also observed experimentally and predicted by AlphaFold2, between the JD and a helix (helix V) in the G/F region (Figure S1). Noticeably, AlphaFold2 also predicted interactions between Sis1's JD and a further distal helix in the G/F linker region (Figure S1, red helix). This structural arrangement is expected to sterically clash with the activatory interaction of the HDP motif in the JD (Figure S1, green) with ATP-Hsp70 in the pocket containing the conserved linker (black), connecting the protein-binding domain to the nucleotide-binding domains (PDB: 5NRO). Interestingly, binding of the EEVD tetrapeptide at the C-terminal end of Ssa1 to the CTD of Sis1 also contributes to the abolition of its autoinhibition.[14,18,33] A similar activatory effect can be achieved by specific mutations (e.g. E50A, or F102A in helix V),[16] or the full deletion of helix V.[16] In yeast Sis1, the presence and role of helix V has not been experimentally determined, albeit its presence is also predicted by AlphaFold2 (Figure S3 and AlphaFold2-resolved structure on Uniprot[40] ID of SIS1: AF-P25294-F1), with contacts with the JD similar to those for DNAJB1.

Our experiments were consistent with these findings, although with some nuanced differences. While the YS chimera, in which the JD–helix V interaction has been putatively abolished by the swap, was constitutively active, even in the absence of the C-terminal EEVD tetrapeptide, its high efficiency at disaggregating and refolding preaggregated luciferase contrasted with results for α-synuclein fibril disaggregation by DNAJB1 and Hsc70, which instead stringently requires EEVD in conjunction with helix V.[16] At this stage we cannot yet assess whether this difference is due to the distinct nature of α-synuclein fibrils with respect to luciferase amorphous aggregates, or to structural features that are not in common between DNAJB1 and Sis1, or because the intramolecular network of autorepressive interactions in class B JDPs is more complex than what has been understood to date.

Remarkably, no autorepression mechanisms have been previously reported for class A JDPs. Here we found that the JD of YY is not fully accessible to Ssa1 for stimulating its ATPase cycle, whereas with the YS chimera, it is fully active. Furthermore, the JD of Ydj1 hinders the substrate-binding efficiency of the CTDs of Ydj1 more than the JD of Sis1, strongly suggesting, once more, the presence of intramolecular interactions between the JDs and CTDs of YY. We also found an anticorrelation between the efficiency at binding and preventing the misfolding (holding) of preunfolded substrates (MlucV), and at leading to their native refolding (Table 1). This result suggested that rather than a generically strong JDP affinity for non-native substrates, what is key to make the Hsp70 machinery functionally efficient at repairing protein structures is instead the tuning of the affinity of JDPs for their substrates by a plethora of different mechanisms (e.g. peptide binding affinity, ability to recognize specific structures and avidity by engineering multiple binding regions), that also allow prompt release from the Hsp70-unfolded polypeptide products.

Last but not least, we also found that the previously reported synergy between class A and B JDPs for protein disaggregation by the Hsp70–Hsp110 system, is absent in the YS/SY mixture, a further and novel indication that their collaboration is not only based on the JD, but more specifically on their intermolecular interactions with their own CTDs. Furthermore, we found that the activity of the YS chimera, the most efficient for Ssa1-mediated luciferase reactivation, closely recapitulates the activity due to the YY/SS synergy, suggesting that the role of the mixture may specifically be to activate the JDs. While we cannot yet pinpoint the precise molecular mechanism behind this effect, our results suggest that the process may be catalytic, where small substoichiometric amounts of one of the JDPs are sufficient to fully activate the activity of the other. This result seems in contrast with a mechanism that would instead be based on specific complexes at defined stoichiometries.

While we have confirmed previously reported autorepressive features of JDPs, and revealed new ones, in this work we have not addressed their precise molecular mechanism. Chemical crosslinking (e.g. using disuccinimidyl suberate)[41,42] followed by digestion and

mass spectrometry could reveal pairs of proximal residues in SS and YY that are absent in the two chimeras. While this approach has been used in the past to investigate the structural basis for the class A/class B synergy,[27] its spatial resolution is limited by the specific choice of crosslinkable residues (e.g. lysines, which are abundant on the surfaces of JDs and CTDs) and the relatively large distance of crosslinking (1–2 nm). Alternatively, using Limited Proteolysis-Mass Spectrometry,[43,44] it could be possible to highlight protein regions that are more protected in the wild-types than in the swap chimeras. FRET or Electron Paramagnetic Resonance pairs suitably positioned on the JDs and on different parts of the CTDs could further provide evidence of the proximity of different portions of these JDPs in single-molecule experiments. Lastly, structural studies (e.g. cryo-electron microscopy) could reveal molecular arrangements that would explain the autorepressed states. In this perspective it is important to stress that, to some extent, our observations could also be compatible with the formation of small JDP oligomers whose structural integrity, albeit volatile, would be based on interactions between the JDs and the CTDs. It is noteworthy that new findings about specific members of these families are revealing their rich structural polymorphism, for example in the form of oligomers of human DNAJA2.[45]

Conclusion

Of course, there remains the background, lingering question: why would have nature evolved JDPs that are less efficient than what would be possible? While we lack a comprehensive perspective of all optimality criteria that lead evolution to specific outcomes, the greater energy efficiency of Sis1 suggests that energy might have been a driving factor, by reducing unnecessary interactions of DNAJAs and DNAJBs with the abundant cytosolic Hsp70s, especially when energy sources are scarce. More research will be needed to uncover all the disparate mechanisms and conditions that control this “stop-and-start mechanism” of JDPs.

Materials and methods

Strains and plasmids

Wild-type *SSA1*, *SSE1*, *SIS1*, *YDJ1,* and swap chimeras were cloned in the pE-SUMOpro vector (1001A: pE-SUMOpro Amp Vector from Life Sensors) for propagation in *E. coli.* The swap chimeras were constructed by PCR by amplifying the 80 first amino acids (JD and a small part of the Glycine-rich region) with the following primers: JYDJ1-F 5′-GCGAACAGATTGGAGGTATGG TTAAAGAA-3′, JYDJ1-R 5′-GCCAGGACC ACCAGG AGCGCCACCAGCAC-3′, JSIS1-F 5′-GCGAACAGATT GGAGGTATGGTCAAGGAG-3′, JSIS1-R 5′-ACCTGGG AATCCGCCACCAAAGCTTGGACCAC-3′) of the two JDPs and insert them inside the vector of the other one using these set of primers (YDJ1V-F 5′-GGCGGATTC CCAGGTGGTGGATTC-3′, YDJ1V-R 5′-ACCTCCAAT CTGTTCGCGGTGAGC-3′, SIS1VF 5′-TGGTCCTGGTG GTCCTGGCGGTGC-3′, SIS1VR 5′-CCAATCTGTTCGC GGTGAGCCTCA-3′) by Gibson Assembly (NEB). All constructs were confirmed by sequencing.

Purification of proteins

For purification of the His10-small ubiquitin-related modifier (SUMO) tagged wild-type SSE1, SSA1, SIS1, YDJ1, and swap chimeras, were expressed and purified from *E. coli* BL21-CodonPlus (DE3)-RIPL cells with IPTG induction (final 0.5 mM for SSA1 and SSE1 and 0.2 for YDJ1, SIS1, and swap chimeras) at 18 °C, overnight. Briefly, cells were grown in LB medium + ampicillin at 37 °C to OD600 ~0.4–0.5. Protein expression was induced by the addition of 0.5 mM IPTG for 3 h. Cells were harvested, washed with chilled PBS, and resuspended in buffer A (20 mM Tris-HCl pH 7.5, 150 mM KCl, 5% glycerol, 2 mM DTT, 20 mM $MgCl_2$) containing 5 mM imidazole, 1 mg/mL Lysozyme, 1 mM PMSF for 1 h. Cells were lysed by sonication. After high-speed centrifugation (16,000 rpm, 30 min/4 °C), the supernatant was loaded onto a gravity flow-based Ni-NTA metal affinity column (2 mL beads, complete His-Tag Purification Resin from Merck), equilibrated and washed with 10 column volumes of buffer A containing 5 mM imidazole. After several washes with high salt buffer A (150 mM KCl, 20 mM Imidazole, and 5 mM ATP), N-terminal His10-SUMO Smt3 tag was cleaved with Ulp1 protease (2 mg/mL), 300 μL, added to beads with buffer (20 mM Tris-HCl pH 7.5, 150 mM KCl, 10 mM MgCl2, 5% glycerol, 2 mM DTT). Digestion of His10 Smt3 was performed on the Ni-NTA resin by, His6-Ulp1 protease. Because of dual His tags, His6-Ulp1 and His10-SUMO display a high affinity for Ni-NTA resin and remain bound to it during cleavage reaction. After overnight digestion at 4 °C, the unbound fraction is collected (which contains only the native proteins). Proteins were further purified by concentrating to ~3 mg/mL and applying to a size exclusion column (Superdex-200 increase, 10/30 GE Healthcare) equilibrated in buffer A containing 5 mM ATP. Pure fractions were pooled, concentrated by ultrafiltration using

Amicon Ultra (Millipore), aliquoted, and stored at −80 °C. All protein concentrations were determined spectrophotometrically at 562 nm using BCA Protein Assay Kit (Reducing Agent Compatible) (cat no. 23250).

The purified proteins were collected, concentrated, and stored at −80 °C for further use.

Luciferase refolding assay

Luciferase activity was measured as described previously.[46,47] In the presence of oxygen, luciferase catalyzes the conversion of D-luciferin and ATP into oxyluciferin, CO_2, AMP, PPi, and hν. Generated photons were counted with a Victor Light 1420 Luminescence Counter from Perkin-Elmer (Turku, Finland) in a 96-well microtiter plate format.

G6PDH refolding assay

Heat-preaggregated G6PDH was refolded by the SSA1 chaperone system as described previously for the DnaK chaperone system,[48] with the following modifications; 500 nM heat-aggregated G6PDH (final concentration) was reactivated in the presence of 6 μM SSA1, incrementing (0–1 μM) JDPs, 0.75 μM SSE1 (the full SSA1 chaperone system) and 5 mM ATP. G6PDH activity was measured at different times of chaperone-mediated refolding reaction at 25 °C.

ATPase assay (Malachite Green)

Colorimetric determination of Pi produced by ATP hydrolysis was performed using the Malachite Green Assay Kit (Sigma-Aldrich, Switzerland) and as described previously.[49] Several concentrations of Hsp70 (SSA1) and JDPs (YY, SS, SY, YS) were mixed with or without substrate (200 nM of preaggregated luciferase) and with 1 mM of ATP and incubated for 1 h at 25 °C. Exactly 4 μL of each sample was taken and put inside a 96-well plate with 76 μL of H_2O. A 20-μL volume of Malachite Green reaction buffer was added, and the samples were mixed thoroughly and incubated at 25 °C for 30 min before measuring at 620 nm on a plate reader (HIDEX-Sense 425–301, Finland). The rate of intrinsic ATP hydrolysis was deduced by subtracting the signal from ATP in the absence of a chaperone.

Light scattering

To monitor the aggregation propensity of urea-denatured Luciferase as described previously,[31] 10 μM Luciferase was denatured with 6 M urea at 30 °C for 10 min, then diluted to a final concentration of 0.3 μM in buffer A (50 mM Tris-HCl pH 7.5, 150 mM KCl, 10 mM $MgCl_2$, 2 mM DTT). The time-dependent aggregation was monitored by light scattering at 340 nm at 30 °C using a PerkinElmer Fluorescence Spectrophotometer.

FRET measurements and FRET efficiency calculation

All ensemble relative FRET efficiencies were calculated from maximum fluorescence emission intensities of the donor (ED) and acceptor (EA) fluorophore by exiting the donor only at 405 nm wavelength.[50,51] Fluorescence emission spectra analysis of MLucV reporter was performed on PerkinElmer LS55 fluorometer. Emission spectra were recorded from 480 to 580 nm wavelength with excitation slit 5 nm and emission slit 10 nm. Average intensity values of spectral crosstalk were minimized by excitation donor at 405 nm. Samples were acquired in the same conditions. The relative FRET efficiencies were calculated using the following equation:

$$FRET_{ensemble} = \frac{E_{acceptor}}{E_{donor} + E_{acceptor}}$$

Normalized FRET efficiencies relative to that of native MLucV were calculated as follows:

$$FRET_{norm} = \frac{FRET_{ensemble} - FRET_{separated}}{FRET_{native} - FRET_{separated}}$$

where $FRET_{ensemble}$ is the measured ensemble FRET efficiency, $FRET_{separated}$ is the calculated ensemble FRET measured in a solution of separated mTFP1 and Venus (0.33) and $FRET_{native}$ is the measured ensemble FRET of native MLucV (0.43). Unless otherwise specified, all ensemble FRET measurements were performed at 400 nM of MLucV. The temperature was maintained at 25 °C unless otherwise specified. All experiments were performed in LRB (20 mM Hepes-KOH pH 7.4, 150 mM KCl, 10 mM $MgCl_2$) refolding buffer containing 5 mM ATP, and 2 mM DTT, unless otherwise specified. Exactly 4 μM BSA was used in assays with chaperones to avoid MLucV species sticking to the vessel, it does not affect the fate of the formed aggregates, nor affects the activity of the chaperones. All experiments were repeated at least three times.

Analysis of protein models

All the models (PDBs) have been analyzed and rendered with the UCSF ChimeraX tool.[52]

Author contribution Conceptualization: MER, PG, PDLR; Methodology: PG, PDLR, MER, BF, ST, AM; Investigation: PG, PDLR, MER, BF, ST, AM; Visualization: PG, PDLR, MER, BF, ST, AM; Supervision: PG, PDLR; Writing—original draft: PG, PDLR, MER; Writing—review & editing: PG, PDLR, MER, BF, ST.

Funding and support Swiss National Science Foundation grants 31003A_175453 and 200020_178763.

Data availability statement All data are available in the main text or supplementary materials.

Declarations of interest The authors declare that they have no known competing financial interests or personal relationships that could have appeared to influence the work reported in this paper.

Appendix A. Supplementary Data

Supplementary data associated with this article can be found online at doi:10.1016/j.cstres.2024.03.008.

References

1. Fauvet B, Rebeaud ME, Tiwari S, De Los Rios P, Goloubinoff P. Repair or degrade: the thermodynamic dilemma of cellular protein quality-control. *Front Mol Biosci.* 2021;8:768888.
2. Sweeney P, Park H, Baumann M, et al. Protein misfolding in neurodegenerative diseases: implications and strategies. *Transl Neurodegener.* 2017;6:6.
3. Rebeaud ME, Mallik S, Goloubinoff P, Tawfik DS. On the evolution of chaperones and cochaperones and the expansion of proteomes across the Tree of Life. *Proc Natl Acad Sci.* 2021;118:e2020885118.
4. Goloubinoff P, Sassi AS, Fauvet B, Barducci A, De Los Rios P. Chaperones convert the energy from ATP into the nonequilibrium stabilization of native proteins. *Nat Chem Biol.* 2018;14:388–395.
5. Zhang R, Malinverni D, Cyr DM, Rios PL, Nillegoda NB. J-domain protein chaperone circuits in proteostasis and disease. *Trends Cell Biol.* 2023;33:30–47.
6. Kampinga HH, Craig EA. The HSP70 chaperone machinery: J proteins as drivers of functional specificity. *Nat Rev Mol Cell Biol.* 2010;11:579–592.
7. Marszalek J, De Los Rios P, Cyr D, et al. J-domain proteins: From molecular mechanisms to diseases. *Cell Stress Chaperones.* 2024;29:21–33.
8. Mayer MP, Kityk R. Insights into the molecular mechanism of allostery in Hsp70s. *Front Mol Biosci.* 2015;2:58.
9. Kampinga HH, Andreasson C, Barducci A, et al. Function, evolution, and structure of J-domain proteins. *Cell Stress Chaperones.* 2019;24:7–15.
10. Kityk R, Kopp J, Mayer MP. Molecular mechanism of J-domain-triggered ATP hydrolysis by Hsp70 chaperones. *Mol Cell.* 2018;69:227–237.e224.
11. Russell R, Karzai AW, Mehl AF, McMacken R. DnaJ dramatically stimulates ATP hydrolysis by DnaK: insight into targeting of Hsp70 proteins to polypeptide substrates. *Biochemistry.* 1999;38:4165–4176.
12. Han W, Christen P. cis-Effect of DnaJ on DnaK in ternary complexes with chimeric DnaK/DnaJ-binding peptides. *FEBS Lett.* 2004;563:146–150.
13. De Los Rios P, Barducci A. Hsp70 chaperones are non-equilibrium machines that achieve ultra-affinity by energy consumption. *Elife.* 2014;3:e02218.
14. Yu HY, Ziegelhoffer T, Osipiuk J, et al. Roles of intramolecular and intermolecular interactions in functional regulation of the Hsp70 J-protein co-chaperone Sis1. *J Mol Biol.* 2015;427:1632–1643.
15. Yan W, Craig EA. The glycine-phenylalanine-rich region determines the specificity of the yeast Hsp40 Sis1. *Mol Cell Biol.* 1999;19:7751–7758.
16. Faust O, Abayev-Avraham M, Wentink AS, et al. HSP40 proteins use class-specific regulation to drive HSP70 functional diversity. *Nature.* 2020;587:489–494.
17. Fan CY, Lee S, Ren HY, Cyr DM. Exchangeable chaperone modules contribute to specification of type I and type II Hsp40 cellular function. *Mol Biol Cell.* 2004;15:761–773.
18. Johnson OT, Nadel CM, Carroll EC, Arhar T, Gestwicki JE. Two distinct classes of cochaperones compete for the EEVD motif in heat shock protein 70 to tune its chaperone activities. *J Biol Chem.* 2022;298:101697.
19. Jiang Y, Rossi P, Kalodimos CG. Structural basis for client recognition and activity of Hsp40 chaperones. *Science.* 2019;365:1313–1319.
20. Wyszkowski H, Janta A, Sztangierska W, et al. Class-specific interactions between Sis1 J-domain protein and Hsp70 chaperone potentiate disaggregation of misfolded proteins. *Proc Natl Acad Sci USA.* 2021;118:e2108163118.
21. Kumar J, Reidy M, Masison DC. Yeast J-protein Sis1 prevents prion toxicity by moderating depletion of prion protein. *Genetics.* 2024;23:100724.
22. Jumper J, Evans R, Pritze A, et al. Highly accurate protein structure prediction with AlphaFold. *Nature.* 2021;596:583–589.
23. Cajo GC, Horne BE, Kelley WL, Schwager F, Georgopoulos C, Genevaux P, et al. The role of the DIF motif of the DnaJ (Hsp40) co-chaperone in the regulation of the DnaK (Hsp70) chaperone cycle. *J Biol Chem.* 2006;281:12436–12444.
24. Wall D, Zylicz M, Georgopoulos C. The conserved G/F motif of the DnaJ chaperone is necessary for the activation of the substrate binding properties of the DnaK chaperone. *J Biol Chem.* 1995;270:2139–2144.
25. Karamanos TK, Tugarinov V, Clore GM. Unraveling the structure and dynamics of the human DNAJB6b chaperone by NMR reveals insights into Hsp40-mediated proteostasis. *Proc Natl Acad Sci.* 2019;116:21529–21538.
26. Ryder BD, Matlahov I, Bali S, Vaquer-Alicea J, vander Wel PCA, Joachimiak LA, et al. Regulatory inter-domain interactions influence Hsp70 recruitment to the DnaJB8 chaperone. *Nat Commun.* 2021;12:946.
27. Nillegoda NB, Kirstein J, Szlachcic A, et al. Crucial HSP70 co-chaperone complex unlocks metazoan protein disaggregation. *Nature.* 2015;524:247–251.
28. Schilke BA, Ciesielski SJ, Ziegelhoffer T, et al. Broadening the functionality of a J-protein/Hsp70 molecular chaperone system. *PLoS Genet.* 2017;13:e1007084.
29. Johnson JL, Craig EA. An essential role for the substrate-binding region of Hsp40s in *Saccharomyces cerevisiae*. *J Cell Biol.* 2001;152:851–856.
30. Shorter J. The mammalian disaggregase machinery: Hsp110 synergizes with Hsp70 and Hsp40 to catalyze protein disaggregation and reactivation in a cell-free system. *PLoS One.* 2011;6:e26319.
31. Tiwari S, Fauvet B, Assenza S, De Los Rios P, Goloubinoff P. A fluorescent multi-domain protein reveals the unfolding mechanism of Hsp70. *Nat Chem Biol.* 2023;19:198–205.
32. Cho H, Shim WJ, Liu Y, Shan SO. J-domain proteins promote client relay from Hsp70 during tail-anchored membrane protein targeting. *J Biol Chem.* 2021;296:100546.
33. Yu HY, Ziegelhoffer T, Craig EA. Functionality of Class A and Class B J-protein co-chaperones with Hsp70. *FEBS Lett.* 2015;589:2825–2830.

34. Lu Z, Cyr DM. Protein folding activity of Hsp70 is modified differentially by the hsp40 co-chaperones Sis1 and Ydj1. *J Biol Chem.* 1998;273:27824–27830.
35. Laufen T, Mayer MP, Beisel C, et al. Mechanism of regulation of hsp70 chaperones by DnaJ cochaperones. *Proc Natl Acad Sci USA.* 1999;96:5452–5457.
36. Mackenzie RJ, Lawless C, Holman SW, et al. Absolute protein quantification of the yeast chaperome under conditions of heat shock. *Proteomics.* 2016;16:2128–2140.
37. Ghaemmaghami S, Huh WK, Bower K, et al. Global analysis of protein expression in yeast. *Nature.* 2003;425:737–741.
38. Lawless C, Holman SW, Brownridge P, et al. Direct and absolute quantification of over 1800 yeast proteins via selected reaction monitoring. *Mol Cell Proteom.* 2016;15:1309–1322.
39. Fauvet B, Finka A, Castanie-Cornet M, et al. Bacterial Hsp90 facilitates the degradation of aggregation-prone Hsp70-Hsp40 substrates. *Front Mol Biosci.* 2021;8:653073.
40. UniProt C. UniProt: a hub for protein information. *Nucleic Acids Res.* 2015;43:D204–D212.
41. Leitner A, Joachimiak LA, Unverdorben P, et al. Chemical cross-linking/mass spectrometry targeting acidic residues in proteins and protein complexes. *Proc Natl Acad Sci.* 2014;111:9455–9460.
42. Manalastas-Cantos K, Adoni KR, Pfeifer M, et al. Modeling flexible protein structure with AlphaFold2 and crosslinking mass spectrometry. *Mol Cell Proteom.* 2024;23.
43. Malinovska L, Cappelletti V, Kohler D, et al. Proteome-wide structural changes measured with limited proteolysis-mass spectrometry: an advanced protocol for high-throughput applications. *Nat Protoc.* 2023;18:659–682.
44. Schopper S, Kahraman A, Leuenberger P, et al. Measuring protein structural changes on a proteome-wide scale using limited proteolysis-coupled mass spectrometry. *Nat Protoc.* 2017;12:2391–2410.
45. Velasco-Carneros L, Cuellar J, Dublang L, et al. The self-association equilibrium of DNAJA2 regulates its interaction with unfolded substrate proteins and with Hsc70. *Nat Commun.* 2023;14:5436.
46. Bischofberger P, Han W, Feifel B, Schönfeld H-J, Christen P. d-Peptides as inhibitors of the DnaK/DnaJ/GrpE chaperone system. *J Biol Chem.* 2003;278:19044–19047.
47. Sharma SK, De los Rios P, Christen P, Lustig A, Goloubinoff P. The kinetic parameters and energy cost of the Hsp70 chaperone as a polypeptide unfoldase. *Nat Chem Biol.* 2010;6:914–920.
48. Mattoo RU, FarinaHenriquez Cuendet A, Subanna S, et al. Synergism between a foldase and an unfoldase: reciprocal dependence between the thioredoxin-like activity of DnaJ and the polypeptide-unfolding activity of DnaK. *Front Mol Biosci.* 2014;1:7.
49. Lee S, Roh SH, Lee J, Sung N, Liu J, Tsai FTF, et al. Cryo-EM structures of the Hsp104 protein disaggregase captured in the ATP conformation. *Cell Rep.* 2019;26:29–36.e23.
50. Fritz RD, Letzelter M, Reimann A, et al. A versatile toolkit to produce sensitive FRET biosensors to visualize signaling in time and space. *Sci Signal.* 2013;6:rs12.
51. Wood RJ, Ormsby AR, Radwan M, et al. A biosensor-based framework to measure latent proteostasis capacity. *Nat Commun.* 2018;9:287.
52. Meng EC, Goddard TD, Pettersen EF, et al. UCSF ChimeraX: tools for structure building and analysis. *Protein Sci.* 2023;32:e4792.e4792.